OPEN

Oncogene (2018) **37**, 174–184

www.nature.com/onc

ORIGINAL ARTICLE

Loss of PRP4K drives anoikis resistance in part by dysregulation of epidermal growth factor receptor endosomal trafficking

DP Corkery[1,2], LE Clarke[2,9], S Gebremeskel[3,9], J Salsman[2], J Pinder[2], C Le Page[4], L Meunier[4], Z Xu[2], A-M Mes-Masson[4,5], JN Berman[2,3,6,7], B Johnston[2,3,7,8] and G Dellaire[1,2,7]

Anoikis acts as a critical barrier to metastasis by inducing cell death upon cancer cell detachment from the extracellular matrix (ECM), thereby preventing tumor cell dissemination to secondary sites. The induction of anoikis requires the lysosomal-mediated downregulation of epidermal growth factor receptors (EGFRs) leading to termination of pro-survival signaling. In this study, we demonstrate that depletion of pre-mRNA splicing factor 4 kinase (PRP4K; also known as PRPF4B) causes dysregulation of EGFR trafficking and anoikis resistance. We also report a novel cytoplasmic localization of PRP4K at the late endosome, and demonstrate both nuclear and cytoplasmic localization in breast, lung and ovarian cancer tissue. Mechanistically, depletion of PRP4K leads to reduced EGFR degradation following cell detachment from the ECM and correlates with increased TrkB, vimentin and Zeb1 expression. As a result, PRP4K loss promotes sustained growth factor signaling and increased cellular resistance to anoikis *in vitro* and in a novel zebrafish xenotransplantation model of anoikis sensitivity, as well as increased metastasis in a mouse model of ovarian cancer. Thus, PRP4K may serve as a potential biomarker of anoikis sensitivity in ovarian and other epithelial cancers.

Oncogene (2018) **37,** 174–184; doi:10.1038/onc.2017.318; published online 11 September 2017

INTRODUCTION

To maintain tissue homeostasis, multicellular organisms regulate the ability of cells to grow and differentiate only when in the correct spatial context within a tissue. Interactions between specific integrin receptors on the cell surface and their extracellular matrix (ECM) counterparts indicate when a cell is in the correct location, transducing signals that promote proliferation and survival.[1–3] When these interactions are lost, cells undergo a form of programmed cell death termed anoikis, which prevents dysplastic cell growth.

Integrins bind the ECM in clusters, resulting in the formation of focal adhesions; large multi-protein structures which form the mechanical link to the ECM and act as a signaling hub to initiate cellular signaling events promoting cell survival, proliferation and migration.[4] Pro-survival signaling from focal adhesions is achieved partially through the coupling of integrin receptors to receptor tyrosine kinases (RTKs). For example, integrin engagement has been shown to induce EGF-independent epidermal growth factor receptor (EGFR) activation resulting in Akt/Erk signaling and anchorage-dependent cell survival.[5] Following loss of integrin engagement, EGFR is trafficked to the lysosome for degradation, leading to the termination of pro-survival signaling.[6,7] This downregulation of EGFR is necessary for anoikis induction as receptor overexpression prevents EGFR downregulation after loss of integrin engagement and promotes anchorage-independent growth.[6] Therefore, understanding the mechanisms that regulate the trafficking and degradation of EGFR following cell detachment will not only further our understanding of anoikis but also identify potential new mechanisms through which cancer cells can evade this detachment-induced apoptotic pathway.

In this study, we identify the pre-mRNA splicing factor 4 kinase (PRP4K) as a novel regulator of anoikis sensitivity. PRP4K is an essential kinase, initially identified in *Schizosaccharomyces pombe* for its role in regulating pre-mRNA splicing,[8] that is evolutionarily conserved from worms to mammals.[9] We recently identified PRP4K as novel HER2/ERBB2-regulated mediator of taxane sensitivity in breast and ovarian cancer.[10] We found that PRP4K levels are decreased in cancer cells that acquired resistance to paclitaxel both *in vitro* and *in vivo*. Importantly, PRP4K protein levels were also decreased in ascites-derived tumor cells isolated from a high-grade serous ovarian cancer patient following relapse from taxane-based therapy, as compared with cells derived from the matched primary tumor at diagnosis. In this study, we identify a novel role for PRP4K in regulating the endosomal trafficking of EGFR leading to altered anoikis sensitivity in epithelial cancer cells. Specifically, loss of PRP4K expression reduced EGF-stimulated EGFR degradation, promoting anchorage-independent cell growth

[1]Department of Biochemistry & Molecular Biology, Dalhousie University, Halifax, Nova Scotia, Canada; [2]Department of Pathology, Dalhousie University, Halifax, Nova Scotia, Canada; [3]Department of Microbiology and Immunology, Dalhousie University, Halifax, Nova Scotia, Canada; [4]Centre de recherche du Centre hospitalier de l'Université de Montréal (CRCHUM) and Institut du cancer de Montréal, Montreal, Quebec, Canada; [5]Département de médecine, Université de Montréal, Montreal, Quebec, Canada; [6]Department of Pediatrics, IWK Health Centre, Halifax, Nova Scotia, Canada; [7]Beatrice Hunter Cancer Research Institute, Halifax, Nova Scotia, Canada and [8]Department of Pediatrics, Dalhousie University, Halifax, Nova Scotia, Canada. Correspondence: Dr B Johnston, Departments of Microbiology and Immunology, Dalhousie University, PO Box 15000, Halifax, Nova Scotia, Canada B3H 4R2 or Dr G Dellaire, Department of Pathology, Dalhousie University, PO Box 15000, Halifax, Nova Scotia, Canada B3H 4R2.
E-mail: brent.johnston@dal.ca or dellaire@dal.ca
[9]These authors contributed equally to this work.
Received 5 August 2016; revised 6 July 2017; accepted 4 August 2017; published online 11 September 2017

in zebrafish xenografts and increased metastasis in a mouse model of ovarian cancer.

RESULTS

Identification and characterization of a cytoplasmic pool of PRP4K localized to the late endosome

In previous studies, PRP4K was demonstrated to localize to the nucleus within SC35-positive 'splicing speckles',[9,11,12] consistent with PRP4K's role in spliceosome assembly.[13] However, immunohistochemistry analysis of PRP4K protein expression in pre-chemotherapy breast, ovarian and lung tumors using tissue microarrays (TMAs) identified both nuclear and a novel cytoplasmic localization of PRP4K (Figure 1a) that was not seen when a peptide was used to block antibody binding (Supplementary Figure 1).

To better evaluate PRP4K subcellular localization *in vitro*, we used a CRISPR/Cas9 mediated knock-in strategy to generate a HeLa cell line (HeLa$^{Clover\text{-}PRP4K}$) expressing the green fluorescent protein clover[14] fused to the N-terminus of PRP4K. In-frame insertion of the clover cDNA was confirmed by western blot analysis using an anti-PRP4K antibody following GFP-affinity purification (Figure 1b), and by genomic sequencing (Supplementary Figures 2 and 3). Western blot analysis indicated that only a single allele was targeted in this cell line. Immunofluorescence analysis of both live and fixed HeLa$^{Clover\text{-}PRP4K}$ cells revealed the expected speckle nuclear localization, but also identified a cytoplasmic pool of PRP4K that increased when cells were treated with 50 μM chloroquine (Figure 1c; Supplementary Figure 4). Given that chloroquine prevents endosomal acidification, leading to late endosome/autophagosome accumulation, the increase in cytoplasmic PRP4K following chloroquine treatment suggested an accumulation of this protein within a late endosomal compartment. To test this hypothesis, HeLa$^{Clover\text{-}PRP4K}$ cells were treated with chloroquine and analyzed for co-localization of endosomal markers via immunofluorescence microscopy (Figure 2). PRP4K co-localized partially with markers of the late endosome (Rab7)[15] and autophagosome (p62),[16] but showed no co-localization with markers of the early endosome (EEA1 and Rab5).[17] In addition, PRP4K-positive cytoplasmic puncta were frequently found adjacent to lysosomes (LAMP2),[18] consistent with a lysosome-endosome fusion defect following chloroquine treatment. Taken together, these data identify a novel cytoplasmic localization for PRP4K with enrichment at the late endosome/autophagosome.

Loss of PRP4K impairs EGFR degradation following EGF stimulation

Given the localization of PRP4K to the late endosome/autophagosome, and the important role of endocytic trafficking in regulating EGFR signaling,[19,20] we sought to determine whether PRP4K was having a role in endocytic trafficking. Stimulation of HeLa$^{Clover\text{-}PRP4K}$ cells with EGF resulted in partial co-localization of PRP4K with activated, internalized EGFR (pEGFR) (Supplementary Figure 5) and the late endosome marker, Rab7 (Supplementary Figure 6). To determine if PRP4K was regulating receptor trafficking, we investigated whether depletion of PRP4K by shRNA could affect EGFR degradation following EGF stimulation. Knockdown of PRP4K in HeLa cells did not impact internalization of the activated

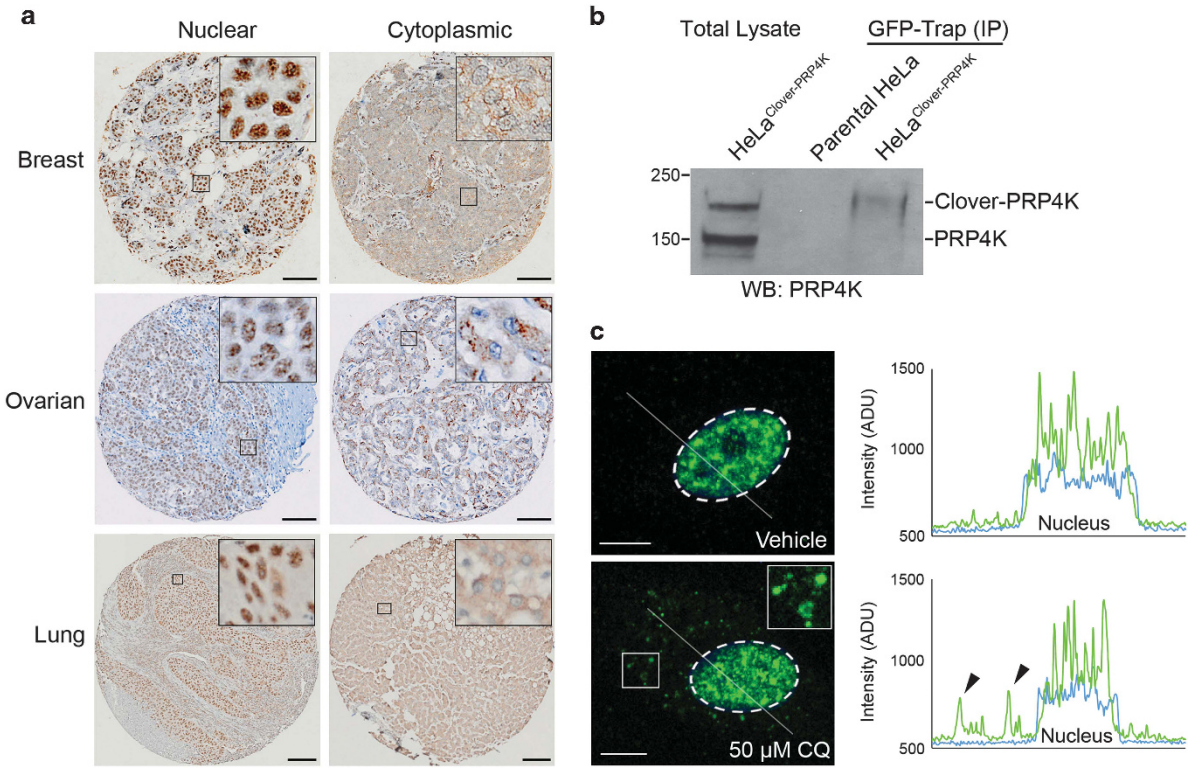

Figure 1. Cytoplasmic localization of PRP4K. (**a**) Representative immunostaining of nuclear and cytoplasmic PRP4K in breast, high-grade serous ovarian and lung cancer tissue microarrays. Scale bars, 100 microns. (**b**) HeLa$^{Clover\text{-}PRP4K}$ cells were generated using a CRISPR/Cas9 mediated knock-in of a clover tag into the *PRPF4B* gene locus. Lysates from parental HeLa and HeLa$^{Clover\text{-}PRP4K}$ cells were subjected to GFP-trap affinity purification and analyzed by western blotting for PRP4K. (**c**) HeLa$^{Clover\text{-}PRP4K}$ cells were treated with vehicle or 50 μM chloroquine (CQ) overnight and analyzed by immunofluorescence confocal microscopy using an anti-GFP antibody (Green). Nuclei were stained with DAPI and indicated by the dashed white line. Scale bars, 10 microns. Solid white line identifies the line scan with the corresponding line plot graph displayed to the right. Green line = PRP4K. Blue line = DAPI. Arrowheads indicate cytoplasmic PRP4K signal.

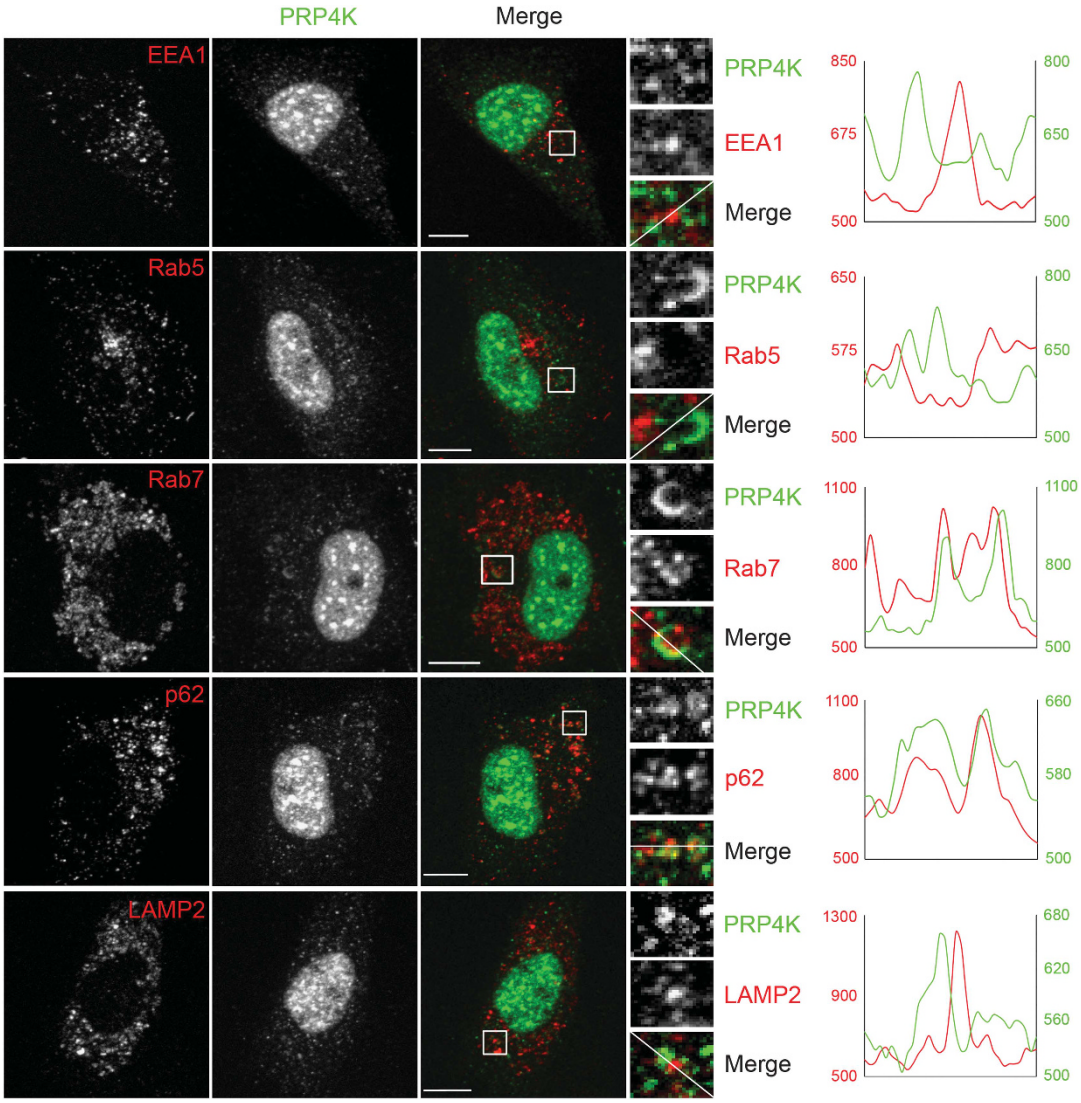

Figure 2. PRP4K co-localizes with markers of the late endosome following chloroquine treatment. To determine whether PRP4K localizes to a component of the endocytic trafficking pathway within the cytoplasm, HeLa$^{Clover\text{-}PRP4K}$ cells were treated with chloroquine overnight and analyzed by immunofluorescence confocal microscopy using antibodies against GFP (green) and the indicated endosomal marker (Red). Whole-cell images are z-stack projections of 20 confocal sections captured at 0.4 μm intervals. Scale bars, 10 microns. White boxes outline the region shown at a higher magnification to the right. Magnified images are shown as a single z-slice. Solid white line identifies the line scan with the corresponding line plot graph displayed to the right. Green line = PRP4K. Red line indicated endosome marker.

EGFR receptor into endosomes but appeared to inhibit its subsequent degradation, as indicated by the significant retention of phospho-EGFR positive endosomes in the cytoplasm of HeLa shPRP4K cells 90 min after stimulation with EGF (Figures 3a and c). Western blot analysis confirmed a delay in the degradation of EGFR (Figures 3b and d) in PRP4K knockdown cells, which resulted in sustained activation of both Erk, as indicated by increased phospho-Erk (T202/Y204) (Figure 3b), and the Akt pathway as indicated by phospho-Akt (S473) (Figures 3b and e). Degradation of EGFR following EGF stimulation has been shown to induce EGFR biosynthesis[21,22] as means of restoring the amount of receptor at the cell surface. Consistent with this, we observed induction of *EGFR* gene expression in response to EGF treatment in HeLa, MCF-7 and ID8 cells (Supplementary Figure 7). However, knockdown of PRP4K in all three cell lines inhibited induction of *EGFR* mRNA, consistent with impaired receptor degradation.

Loss of PRP4K increases cellular resistance to anoikis *in vitro*

The induction of anoikis following ECM detachment is a complex process which includes the downregulation of EGFR leading to the termination of pro-survival signaling via Akt and Erk.[6] Cancer cells which have lost the ability to downregulate EGFR[6] and human keratinocytes stimulated with EGF[23] both escape anoikis when cultured under non-adherent conditions, demonstrating the importance of EGFR activation in anchorage-independent cell growth. Given the EGFR trafficking defect in PRP4K-depleted HeLa cells, we next sought to determine whether PRP4K knockdown could rescue cells from anoikis using ID8 mouse ovarian cancer (Figure 4a) and MCF-7 breast cancer cells (Figure 5a). Although we observed no difference in proliferation of adherent control and knockdown cells (Figures 4b and 5b) or in the expression of Bcl2 or Bcl-xL (Figures 4c and 5c) in either ID8 or MCF-7 cells, loss of PRP4K in ID8 cells under non-adherent conditions resulted in

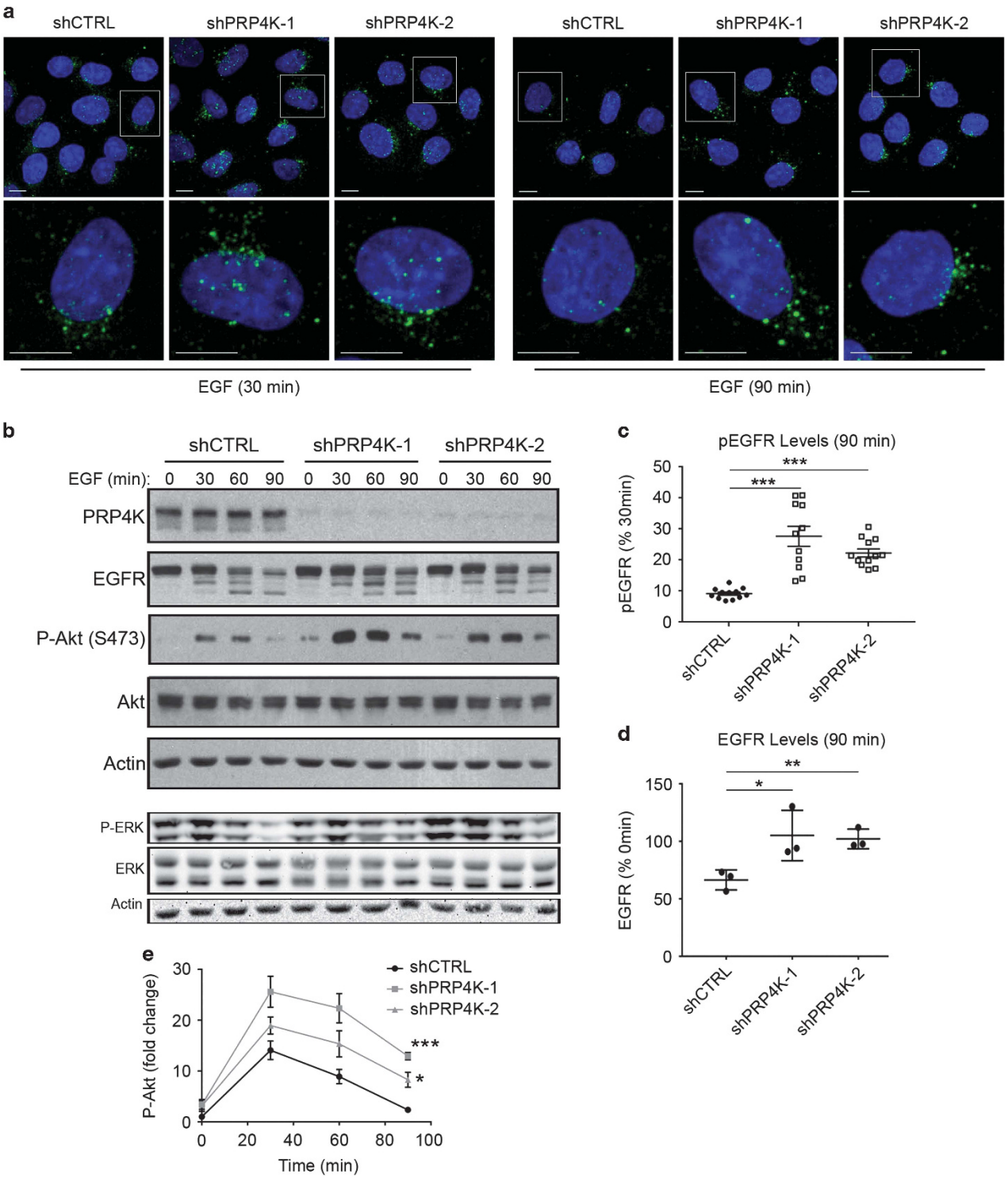

Figure 3. PRP4K regulates EGF-dependent EGFR degradation. (**a**) HeLa shCTRL, shPRP4K-1 and shPRP4K-2 cells were serum starved overnight and treated with 50 ng/ml EGF for 30 and 90 min. Cells were fixed and analyzed by immunofluorescence confocal microscopy using an antibody against phospho-EGFR (green). Nuclei were stained with DAPI (blue). White boxes outline the cell shown at an increased magnification directly below. Scale bars, 10 microns. (**b**) HeLa shCTRL, shPRP4K-1 and shPRP4K-2 cells were serum starved overnight and treated with 50 ng/ml EGF for the indicated time period. Whole-cell lysates were prepared and subject to western blot analysis using the indicated antibodies. (**c**) Cytoplasmic phospho-EGFR (pEGFR) levels (90 min post-EGF stimulation) where quantified by immunofluorescence microscopy as a percentage of pEGFR staining at 30 min post EGF in each cell line. The points in the scatterplots represent the sum of the mean fluorescence intensity of all cytoplasmic pEGFR puncta per cell from 12 fields of view (z-stack projections of 20 confocal sections captured at 0.4 μm intervals) across three experiments, where each field of view contained 20–25 cells. Error bars = s.e.m. $^{***}P < 0.001$. (**d**) EGFR protein levels (90 min post-EGF stimulation) were quantified using densitometry from western blots and normalized as a percentage of EGFR levels at 0 min in HeLa shCTRL, shPRP4K-1 and shPRP4K-2 cells. Scatterplots represent data from three independent experiments. Error bars = s.d. $^{*}P < 0.05$; $^{**}P < 0.01$. (**e**) P-Akt levels were quantified using densitometry and represented as the mean from three independent experiments. Error bars = s.d. $^{*}P < 0.05$; $^{***}P < 0.001$.

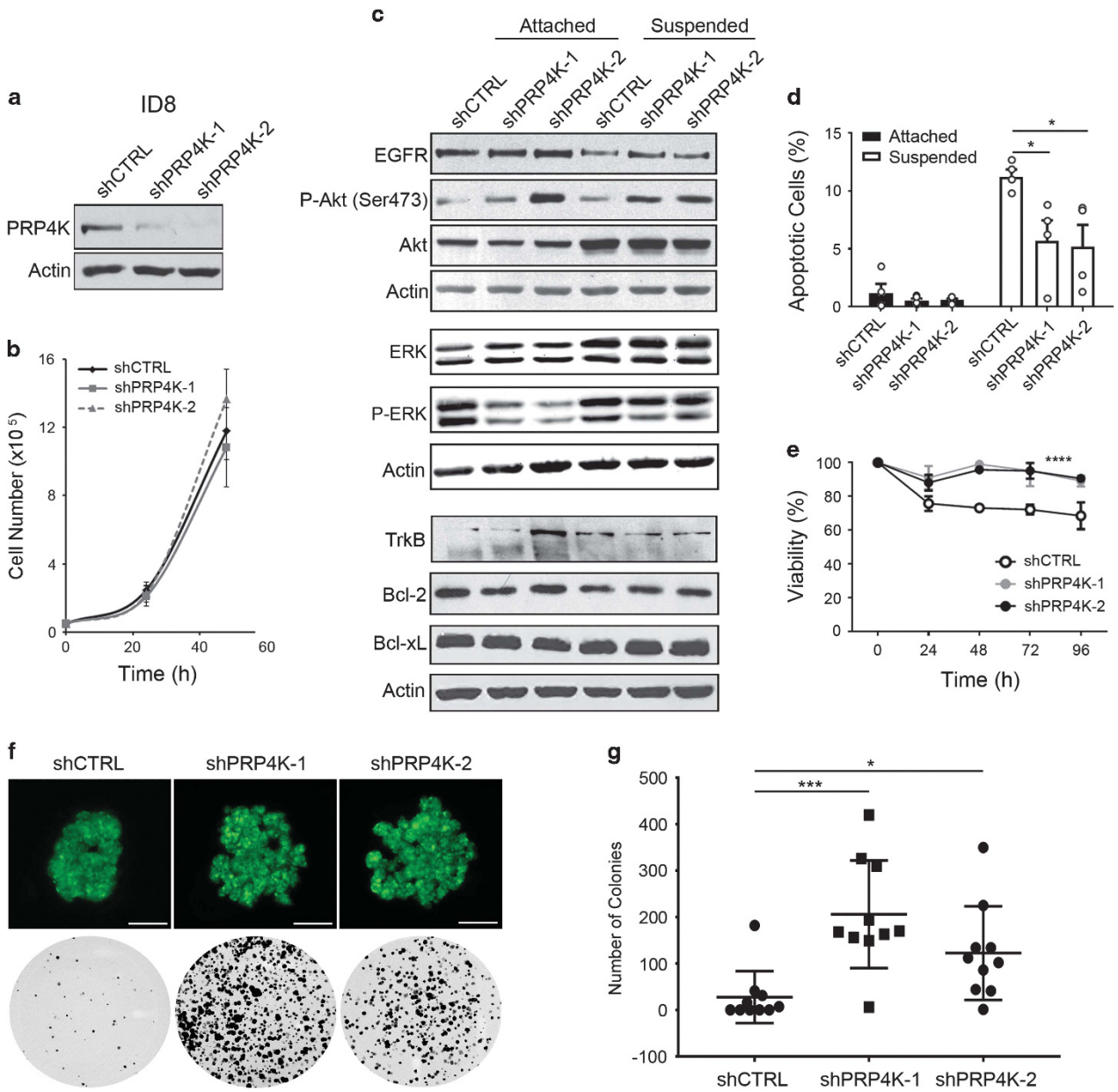

Figure 4. Loss of PRP4K promotes anoikis resistance in ID8 ovarian cancer cells via sustained RTK signaling. (**a**) ID8 cells were transduced with control or PRP4K targeting shRNA lentiviral vectors to generate cell lines stably expressing the indicated hairpin. Knockdown of PRP4K was confirmed by western blot analysis. (**b**) *In vitro* proliferation rates were determined by plating 50 000 cells for each cell line and performing cell counts every 24 h. Data are presented as mean of four independent experiments ± s.d. (**c**) ID8 shCTRL and shPRP4K cells lines were cultured as attached monolayers or suspended on polyHEMA coated plates for 24 h. Cells were harvested and subject to western blot analysis using the indicated antibodies. (**d**) The frequency of apoptotic cells in adherent and suspension growth conditions after 24 h was quantified by flow cytometric Annexin-V staining. Error bars = s.e.m. ($N = 4$). *$P < 0.05$ (**e**) Cell viability was also ascertained in non-adherent conditions relative to adherent cell growth over 72 h via AlamarBlue staining. Error bars = s.d. ($N = 4$). Significance was determined by a two-way ANOVA ****$P < 0.0001$ (**f**) Representative images of ID8 spheroids after 7 days in culture (top). Scale bars, 250 μm. Individual spheroids were harvested, trypsinized, and plated in 6-well plates. After 5 days in culture, colonies were fixed and stained with crystal violet. Representative images show colony growth for each of the three cell lines (bottom). (**g**) Stained colonies from three independent experiments were counted using ImageJ and represented as the mean colony number. Error bars = s.d. *$P < 0.05$; ***$P < 0.001$.

sustained Akt pathway activation (Figure 4c), reduced apoptosis (Figure 4d) and increased viability (Figure 4e), as well as enhanced anchorage-independent growth as multicellular spheroids (Figures 4f and g). Although we did not see a difference in Akt phosphorylation between control and PRP4K-depleted MCF-7 cells when grown in non-adherent conditions, PRP4K knockdown cells did exhibit anoikis resistance as evidenced by reduced apoptosis (Figure 5d) and increased viability in suspension (Figure 5e).

To determine if trafficking of other RTKs was impacted by the loss of PRP4K, we examined protein levels of TrkB, a known driver of anoikis resistance.[24] Knockdown of PRP4K in both ID8 (Figure 4c) and MCF-7 (Figure 5c) cells was associated with increased TrkB levels. Since TrkB overexpression can contribute to

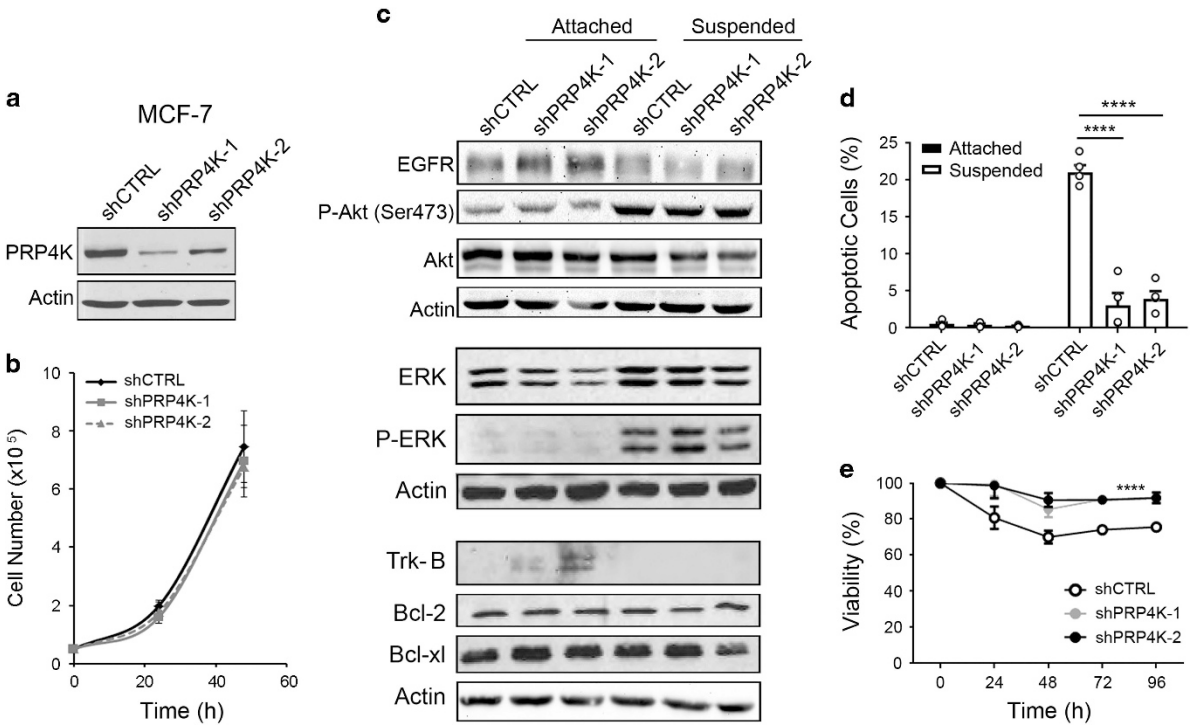

Figure 5. Loss of PRP4K promotes anoikis resistance in MCF-7 breast cancer cells. (**a**) MCF-7 cells were transduced with control or PRP4K targeting shRNA lentiviral vectors to generate cell lines stably expressing the indicated hairpin. Knockdown of PRP4K was confirmed by western blot analysis. (**b**) *In vitro* proliferation rates were determined by plating 50 000 cells for each cell line and performing cell counts every 24 h. Data are presented as mean of four independent experiments ± s.d. (**c**) MCF-7 shCTRL and shPRP4K cells lines were cultured as attached monolayers or suspended on polyHEMA coated plates for 24 h. Cells were harvested and subject to western blot analysis using the indicated antibodies. (**d**) The frequency of apoptotic cells in adherent and suspension growth conditions after 24 h was quantified by flow cytometric Annexin-V staining. Error bars = s.e.m. ($N = 4$). ****$P < 0.0001$. (**e**) Cell viability was also ascertained in non-adherent conditions relative to adherent cell growth over 72 h via AlamarBlue staining. Error bars = s.d. ($N = 4$). Significance was determined by a two-way ANOVA ****$P < 0.0001$.

epithelial-to-mesenchymal transition (EMT) and is associated with increased expression of EMT-markers vimentin, Snail and Zeb1,[25,26] we also surveyed the expression of these and other markers of EMT in control and PRP4K-depleted ID8, MCF-7 and HeLa cells (Supplementary Figure 8). Consistent with upregulation of TrkB, we observed increased expression of Zeb1 in all three cell lines after PRP4K depletion, and vimentin in at least 1 of 2 knockdown lines in ID8 and HeLa cells.

Knockdown of PRP4K increases survival and growth of ID8 cells in zebrafish embryos

To explore the anoikis resistance phenotype associated with knockdown of PRP4K *in vivo*, we employed a zebrafish xeno-transplantation model.[27] In this model, human cancer cells are transplanted into the yolk sac of zebrafish embryos at 48 h post fertilization. The yolk sac provides a nutrient-rich acellular environment in which engrafted cells are suspended and, unlike engraftment in tissue, lacks the necessary ECM contacts required to prevent anoikis. ID8 shCTRL and ID8 shPRP4K cells were transplanted into 48 h old zebrafish embryos and cell proliferation visualized by imaging individual embryos at 24 and 72 h post injection (Figure 6a). Cell growth and proliferation were quantified *ex vivo* in pools of dissociated embryos using fluorescence microscopy.[27] Over 48 h post injection, ID8 shCTRL cells grew poorly within embryos, as expected for an anoikis-sensitive epithelial cell line. In contrast, we observed a ~2-fold increase in ID8 shPRP4K cell number over the same time period (Figure 6b), consistent with an increased *in vivo* resistance to anoikis in PRP4K-depleted ID8 cells.

Knockdown of PRP4K enhances peritoneal dissemination in a syngeneic mouse model of epithelial ovarian cancer

Acquisition of anoikis resistance is an essential prerequisite for tumor metastasis, particularly in the peritoneal dissemination of ovarian cancer cells.[28] To determine if the increased resistance to anoikis associated with loss of PRP4K *in vitro* was sufficient to promote dissemination in a mouse model of ovarian cancer, ID8 shCTRL and ID8 shPRP4K cells were injected intraperitoneally into mice and the frequency of tumor nodules and tumor cells in the ascites fluid was assessed 28 days later. Mice injected with ID8 shPRP4K cells had an increased number of metastatic nodules on the diaphragm and peritoneal wall (Figures 7a–c) and also had an increased number of GFP-positive tumor cells present within the ascitic fluid (Figure 7d). In separate experiments, ID8 shCTRL cells were recovered from the ascites of mice 28 days post injection and examined for their sensitivity to anoikis (Figures 7e–g). As described by Cai and colleagues,[29] ID8 cells isolated from ascites exhibited increased anoikis resistance, which correlated with reduced PRP4K levels and increased Akt phosphorylation in cell lines rescued from 3 of the 4 injected mice (Figure 7h). Similarly, we observed a reduction in PRP4K levels in cells isolated from ascites in 3 out of 4 ovarian cancer patients, relative to their primary tumor (Figure 7i). Finally, we observed increased TrkB, vimentin and Bcl2 expression in the all of the ascites-derived ID8 cell lines (Figure 7h). Together these data indicate that depletion of PRP4K can increase ovarian cancer metastasis, and that loss of PRP4K can also occur as a consequence of adaptation of ovarian cancer cells to non-adherent growth *in vivo*, consistent with PRP4K loss playing a role in anoikis resistance. Furthermore, given its role in suppressing anoikis resistance, these data may explain why

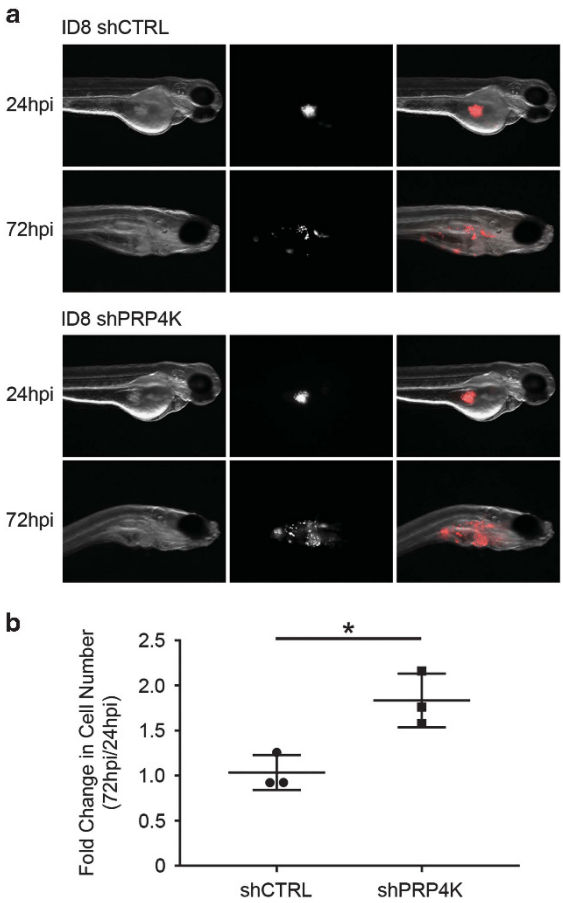

Figure 6. Knockdown of PRP4K increases ID8 proliferation in a zebrafish xenotransplantation model. (**a**) Representative brightfield, fluorescent and merged images are shown for zebrafish embryos at 24 and 72 h post injection (hpi) with either ID8 shCTRL or ID8 shPRP4K-1 cells. (**b**) ID8 shCTRL and shPRP4K-1 engrafted embryos were dissociated at 24 and 72 hpi and the number of fluorescent cells counted. The fold change in cell number was determined and represented as a scatterplot with each point representing an independent experiment. Pooled groups of 15–20 embryos were used for each data point. Error bars = s.d. $*P < 0.05$.

overexpression or amplification of *PRPF4B* gene is associated with significantly better overall survival in patients with high-grade serous ovarian cancer (Figure 8).

DISCUSSION

Anoikis acts as a critical barrier to metastasis by inducing apoptosis in tumor cells which have detached from the primary tumor.[30] The disengagement of integrins during detachment from ECM reduces EGFR expression, resulting in suppression of pro-survival signaling,[6,7] a step necessary for the induction of anoikis. As such, increased expression or activity of EGFR is a common mechanism through which tumor cells evade anoikis.[6,23,31,32] Furthermore, since both EGFR and integrins are capable of signaling from the endosome,[33,34] trafficking defects which prevent receptor degradation and promote endosomal enrichment following cell detachment can influence anoikis susceptibility.[34,35] Here, we identify the splicing kinase PRP4K as a novel regulator of EGFR trafficking, where loss of PRP4K is associated with impaired endosomal trafficking and degradation of EGFR resulting in anoikis resistance *in vitro* and *in vivo*. Thus, we propose that loss of PRP4K could represent a novel biomarker for anoikis resistance in epithelial cancers.

Cytoplasmic PRP4K localizes to the late endosome and its depletion impairs endosomal trafficking of growth factor receptors leading to Akt activation

PRP4K had initially been reported to localize exclusively in the nucleus with enrichment at SC35-containing splicing speckles.[9,11,12] Despite being a nuclear protein during interphase, a cytoplasmic role for this kinase outside of mRNA splicing had been revealed by the study of cells in mitosis, where PRP4K is believed to regulate the spindle assembly checkpoint.[12] In the current study, we employed CRISPR-mediated gene editing to insert a clover fluorescence tag into the *PRPF4B* gene, enabling direct visualization of PRP4K localization without the limitations associated with indirect immunofluorescence, such as issues with antibody penetration and epitope masking. With this approach, we revealed a novel cytoplasmic localization for PRP4K (Figure 1) with enrichment at late endosomes marked by Rab7 (Figure 2; Supplementary Figure 6). Functionally, we have identified a novel role for PRP4K in the trafficking of EGFR, where PRP4K co-localizes in endosomes containing phospho-EGFR (Supplementary Figure 5), and depletion of PRP4K leads to an endosomal accumulation and reduced degradation of EGFR following EGF stimulation (Figure 3). This reduction in receptor degradation resulted in an increased and sustained activation of the Akt and Erk pathways (Figures 3b and d), which provides a mechanism by which PRP4K-depleted cells overcome anoikis.[36,37] The activation of Akt by depletion of PRP4K resembles recent results observed following the knockdown of another splicing kinase, SRSF protein kinase 1 (SRPK1).[38] In the SPRK1 study, sustained Akt activation was observed following EGF stimulation in SRPK1 knockout mouse embryonic fibroblasts (MEFs). Similar to PRP4K-depleted ID8 and MCF-7 cells, SRPK1 knockout MEFs also displayed increased anchorage-independent growth.[38] This study by Wang and colleagues also revealed a splicing-independent role for SPRK1, where loss of SRPK1 promoted Akt activation by affecting the interaction of the Akt phosphatase PH domain and leucine rich repeat protein phosphatase 1 (PHLPP1) with Akt. Thus, by affecting endosomal trafficking of growth factor receptors, PRP4K loss appears to activate Akt in a different manner than reported for loss of SRPK1. In addition, in both ID8 and MCF-7 cells, PRP4K depletion triggered an increase in TrkB (Figures 4c and 5c); a known regulator of anoikis resistance.[24] Thus, increased TrkB signaling may also contribute to the anoikis resistance observed with PRP4K loss.

Finally, both PRP4K and SRPK1 have roles in alternative splicing by phosphorylating splicing factors.[39,40] SPRK1 exhibits both a nuclear and cytoplasmic localization, with the cytoplasmic pool being responsible for the phosphorylation of serine/arginine (SR)-proteins, which in turn regulates their nuclear-cytoplasmic shuttling.[41–43] The novel cytoplasmic localization for PRP4K reported here, the ability of both PRP4K and SRPK1 loss to activate Akt, combined with the known redundancy in SR-protein substrates between the splicing kinases,[39,44] raises the intriguing possibility that these two kinases may share some degree of functional redundancy that extends beyond the regulation of splicing.

Loss of PRP4K: implications for ascites development, metastasis and treatment resistance in recurrent ovarian cancer

More than one third of ovarian cancer patients present with an accumulation of peritoneal ascites at the time of diagnosis.[45–48] The accumulation of ascites is believed to result in part from a combination of altered vascular permeability within the tumor microvasculature[49] and tumor-mediated obstruction of lymphatic drainage.[50] Management of ascites is generally limited to treatment of the underlying disease with platinum and taxane-based chemotherapy. While the clinical response to first-line chemotherapy is quite high, ranging from 70 to 80%,[51–53] the

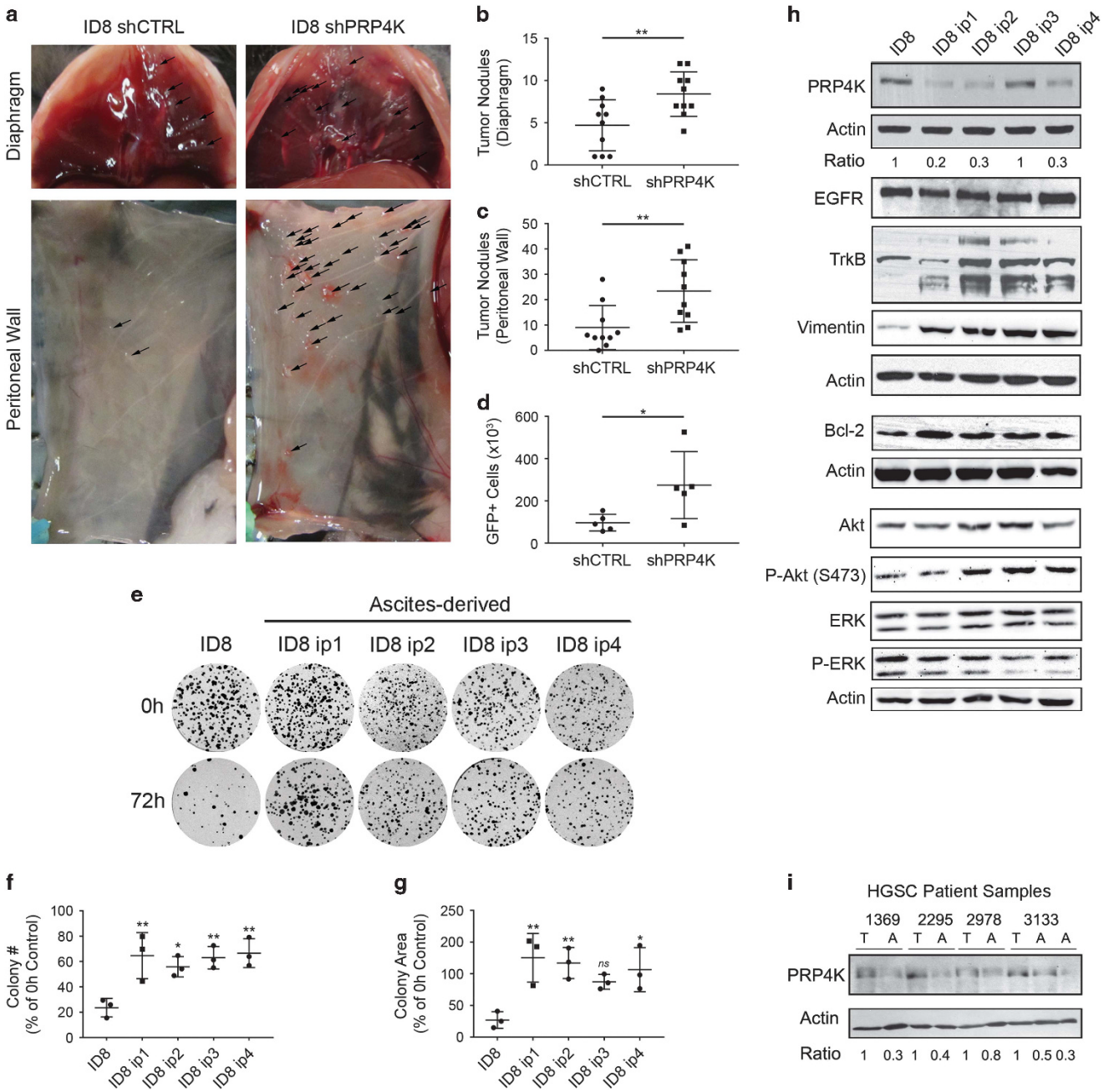

Figure 7. Knockdown of PRP4K increases metastasis in a syngeneic mouse model of ovarian cancer. (**a**) Representative images of tumors on the diaphragm and peritoneal wall of mice at 28 days post injection (dpi) with ID8 shCTRL or ID8 shPRP4K cells. (**b**,**c**) Tumor nodules on the diaphragm and peritoneal wall were quantified in two independent experiments using 5 mice per group. (**d**) Ascites fluid was harvested from five ID8 shCTRL and five ID8 shPRP4K injected mice at 28 dpi and the number of GFP^+ cells was quantified by flow cytometry. (**e**) GFP^+ ID8 cells were recovered at 28 dpi from individual mice injected with ID8 shCTRL cells (ID8 ip1-4). Cells were cultured under non-adherent conditions for 0 or 72 h and re-plated on adherent 6-well plates. Representative images show colony growth for each cell line. (**f**,**g**) Colony number and colony area of ascites-derived ID8 cells grown under non-adherent conditions were quantified relative to adherent conditions for three independent experiments. (**h**) Total cell lysates were prepared from ID8 and ID8 ip cell lines and subjected to western blot analysis for the indicated proteins. (**i**) Western blot analysis of PRP4K protein levels in patient-derived primary high-grade serous ovarian cancer (HGSC) tumors 'T' and matched ascites 'A', where the relative levels of PRP4K between tumor and ascites is indicated (Ratio) after normalization to actin. $*P < 0.05$; $**P < 0.01$; ns = not significant.

majority of patients (50–75%) relapse due to the development of chemoresistance.[54] In most cases, recurrent disease is accompanied by intractable ascites that likely arises from increased peritoneal transcoelomic metastases and requires frequent paracentesis for temporary relief of symptoms.[46]

Our previous study identified PRP4K as a HER2-regulated modifier of taxane sensitivity in breast and ovarian cancer.[10] PRP4K levels were shown to decrease in cells that had acquired resistance to taxanes, both *in vitro* and *in vivo*. In addition, our previous study demonstrated that low PRP4K expression in ovarian tumors was strongly associated with disease progression and poor survival outcomes in a cohort of taxane-treated serous ovarian cancer patients with low HER2 receptor expression. Data provided in the current study demonstrated that depletion of

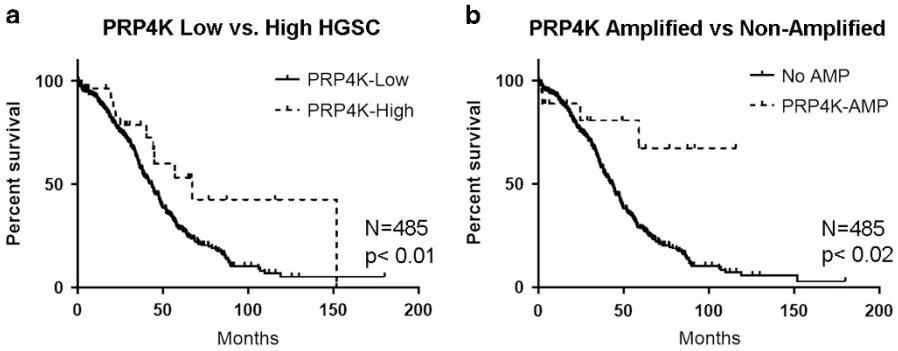

Figure 8. Overexpression or amplification of PRP4K (*PRPF4B*) correlates with significantly increased overall survival in high-grade serous ovarian cancer (HGSC). Kaplan–Meier analyses of data from the TCGA ovarian cancer study[56] (accessed from the http://www.cbioportal.org/ on June 3, 2017)[65] indicating significantly better overall survival in HGSC patients with tumors that (**a**) overexpress *PRPF4B* ($N = 29$ with > 2 s.d. expression of *PRPF4B* relative to the mean; $P < 0.02$ hazard ratio of 2.0 (95% confidence interval (CI): 1.3 to 3.1)), or (**b**) harbor amplifications of the *PRPF4B* gene ($N = 18$; $P < 0.01$ hazard ratio of 3.5 (95% CI: 2.0 to 6.1).

PRP4K protein levels increased cellular resistance to anoikis in zebrafish ovarian cancer xenografts (Figure 6) and promoted metastasis in the ID8 mouse model of ovarian cancer (Figures 7a–d). Furthermore, we found that cancer cells harvested from the ascites of 3 out of 4 mice, and 3 out of 4 human patients with ovarian cancer, exhibited reduced PRP4K expression (Figures 7h–i), and that the ID8 ascites-derived mouse ovarian cancer cells had increased survival under non-adherent growth conditions *in vitro* (Figures 7e–h). These results mirror the associated loss of PRP4K expression in cancer cell lines treated with taxanes *in vitro* and in patient tumors following taxane treatment.[10] Combining our previous work with the current study, we believe we have uncovered one potential mechanism whereby acquired resistance to taxanes through the loss of PRP4K is accompanied by increased anoikis resistance that could in turn promote transcoelomic metastasis and ascites development. In agreement with a possible tumor suppressor role of PRP4K in ovarian cancer, analysis of TCGA data[56] indicated that both amplification of the *PRPF4B* gene and its overexpression (> 2 SD from the mean) were associated with significantly better overall survival (Figure 8). As such, future clinical studies employing PRP4K as a biomarker for prediction of ovarian cancer progression and survival post-taxane therapy may be warranted.

MATERIALS AND METHODS

Patient samples, TMA and immunohistochemistry

Patient-derived cell lines from primary tumors and ascites were described previously.[57] PRP4K staining of the breast and ovarian cancer TMAs has also been described previously,[10,58] and lung staining was carried out as described in Corkery *et al*.[10] The ovarian and breast studies were approved by the institutional ethics board at the Université de Montréal (Montreal, Canada), and the lung study was approved by the ethics committee of the Queen Elizabeth II (QEII) Hospital/Nova Scotia Health District (Halifax, Canada). Tumors were collected and banked following appropriate written consent from patients undergoing surgery within the hospital sites. The ovarian cancer TMA was made using 196 high-grade serous ovarian cancer tumor cases in duplicate cores of 0.6 mm diameter. The breast cancer TMA was made using 150 cases of breast cancer. The lung cancer TMA consisted of 332 tumors taken from primary surgical cases of non-small cell lung cancer including adenocarcinoma (60%), squamous cell carcinoma (37%), and both large cell carcinoma and large cell neuroendocrine carcinoma (3%).

Cell culture and shRNA lentiviral transduction

HeLa (ATCC) and ID8 (Dr Paul Terranova, University of Kansas Medical Center[59]) cells were cultured in Dulbecco's modified Eagle's medium (Sigma, Oakville, ON, Canada) supplemented with 10% fetal calf serum, 1% penicillin/streptomycin at 37 °C with 5% CO_2. To generate the ID8 GIPZ shPRP4K and HeLa TRIPZ shPRP4K cell lines, GIPZ (shPRP4K-1 = clone: V3LMM_463188, shPRP4K-1 = clone: V3LMM_463189, Non-silencing shCTRL = RHS4346) and TRIPZ (shPRP4K-1 = clone: V2THS_47787, shPRP4K--2 = clone: V3THS_383960, Non-silencing shCTRL = RHS4743) lentiviral shRNAs were purchased from Thermo Scientific (Burlington, ON, Canada). Lentivirus was produced by co-transfection of the GIPZ/TRIPZ plasmids with pMD2.G, pCMV-8.92 and pCMV-8.93 lentiviral packaging vectors into human HEK-293 T cells via calcium-phosphate transfection (Promega, Madison, WI, USA) as described previously.[60] After 48 h, viral media from the transfected cells was filtered (0.45 μ filter) added to the target cells for 24 h, after which cells were allowed to recover for 24 h in fresh media before selection in media containing 2 μg/ml puromycin for 4–5 days. To induce expression of the TRIPZ PRP4K shRNA in HeLa cells, 2 μg/ml doxycycline was added to culture media for 72–96 h before experimentation with the drug being replaced every 24 h.

MCF-7 shCTRL and shPRP4K-1 and 2 cell lines are described in detail in.[10] For EGF stimulation, HeLa shCTRL/shPRP4K cells were serum starved overnight using DMEM containing 0.25% FBS, followed by treatment with 50 ng/ml EGF (Sigma) for the indicated time period.

Generation of the HeLa$^{Clover\text{-}PRP4K}$ cell line

The cDNA for the GFP variant clover (gift from Michael Lin, Addgene plasmid # 40259)[14] was inserted into exon 1 of the *PRPF4B* gene after the codon encoding the third amino acid of the PRP4K protein using a similar Cas9-based knock-in strategy as previously described[61] (Supplementary Figures 1 and 2). Briefly, HeLa cells were nucleofected using the Neon® transfection system (Thermo Scientific), according to the manufacturer's directions cells, with the pX335-U6-Chimeric_BB-CBh-hSpCas9n(D10A) (gift from Feng Zhang, Addgene plasmid # 42335)[62] encoding two paired sgRNA's targeting the *PRPF4B* locus (Supplementary Figure 2), along with a homology donor plasmid encoding 130 nucleotides of homology to the *PRPF4B* flanking the cDNA for Clover (Supplementary Figure 1) cloned into pCR2.1 (Thermo Scientific). Individual clones were isolated by limiting dilution, screened for green fluorescence, and characterized by genomic PCR of the *PRP4FB* gene using primers to amplify the edited locus (Supplementary Figure 2) and sequencing of the PCR amplicon (Genewiz, South Plainfield, NJ, USA).

Western blot analysis

Cells were lysed in ice-cold lysis buffer (20 mM Tris-HCl pH8, 300 mM KCl, 10% Glycerol, 0.25% Nonidet P-40, 0.5 mM EDTA, 0.5 mM EGTA, 1× protease inhibitors) and lysates cleared by centrifugation (25 min, 15 000 × *g*, 4 °C) before PAGE and western blotting as previously described.[10] Primary antibodies used for western blot analysis were used at the dilution recommended by the manufacturer unless noted, and included a custom PRP4K antibody (H143, 1:1000);[9] antibodies from Cell Signaling (Danvers, MA, USA), anti-EGFR (#4267, 1:2000), anti-Akt (pan) (#4691, 1:2000), anti-p-Akt (Ser473) (#4060, 1:2000), anti-Erk (#4695), anti-pErk (#9106), anti-Bcl2 (#3498) and antibodies in the EMT sampler kit (#9782); Sigma, anti-actin (A2228) (1:5000); and Santa Cruz (Santa Cruz, CA, USA), anti-TrkB (sc-37721). Secondary antibodies used include HRP-conjugated goat anti-rabbit IgG (Sigma, A6154), HRP-conjugated sheep

anti-mouse IgG (Sigma, A5906) and HRP-conjugated donkey anti-sheep IgG (Sigma, A3415).

Immunofluorescence microscopy and live-cell imaging

HeLa$^{Clover\text{-}PRP4K}$ cells were plated onto glass coverslips in a 6-well plate and treated overnight with 50 μM chloroquine (Sigma) or stimulated with EGF as above. Cells were fixed with 4% paraformaldehyde in PBS for 10 min at room temperature, permeabilized with 0.1% Triton X-100 in PBS for 10 min and immunolabeling was carried out as previously described.[10] Fluorescent images were captured with a Zeiss Cell Observer spinning-disk microscope (Intelligent Imaging Innovations, 3i, Boulder, CO, USA) using a 1.4 NA 63× immersion oil objective lens. Images were processed using only linear adjustments in Adobe Photoshop CS5 and Slidebook (3i) software, which was also used for the analysis of mean fluorescence intensity of immunostaining.

Antibodies used for immunofluorescence were used at the manufacturers recommended dilution unless otherwise noted, and include anti-GFP (Abcam, Toronto, ON, Canada, ab13970) (1:2000 dilution), anti-EEA1 (Cell Signaling, #3288) (1:100 dilution), anti-Rab5 (Cell Signaling, #3547) (1:200 dilution), anti-Rab7 (Cell Signaling, #9367) (1:100 dilution), anti-p62 (Cell Signaling, #7695) (1:400 dilution), anti-LAMP2 (Abcam, ab25631) (1:200 dilution), and anti-p-EGFR (Tyr1068) (Cell Signaling, #3777) (1:800 dilution).

Quantification of *in vitro* proliferation rates

To determine the *in vitro* proliferation rates of ID8 and MCF-7 shCTRL, shPRP4K-1 and shPRP4K-2 cells, 50 000 cells were plated in individual wells of a 6-well plate. Cells were trypsinized and counted at 24 and 48 h after plating.

Spheroid cell growth, viability and anoikis assays

Spheroids assays were conducted in 6-well plates as described previously[63] and images of each well were captured with a digital camera and the number of colonies quantified using ImageJ (NIH, Bethesda, MA, USA). For anoikis assays, poly 2-hydroxyethyl methacrylate (PolyHEMA) (Sigma, P3932) was dissolved in 95% ethanol (20 mg/ml) at 65 °C and used to coat tissue culture plates (4 ml per 10 cm plate) dried overnight at 37 °C. Cells were plated on PolyHEMA coated and non-coated tissue culture dishes for 24 h and then harvested for western blot analysis, cell viability assays using AlamarBlue (DAL1100, Life Technologies, Mississauga, ON, Canada),[10] and apoptosis assays using allophycocyanin-conjugated Annexin-V (eBioscience, Mississauga, ON, Canada) and flow cytometry (FACSCalibur flow cytometer, BD Biosciences, Mississauga, ON, Canada) as described previously.[64] Flow cytometry data was analyzed using FlowJo (V10.2; FlowJo, Ashland, OR, USA).

Zebrafish xenotransplantation

All zebrafish studies were approved by the Dalhousie University Committee on Laboratory Animals. ID8 shCTRL or ID8 shPRP4K cells labeled with the lipophilic cell tracking dye, CM-DiI (Thermo Scientific) were injected (25–50 cells) into the yolk sac of 48 h *casper* zebrafish embryos. Embryos were imaged and enzymatically dissociated to quantify cancer cell growth at 24 and 72 h post injection as described previously.[27]

Mouse experiments

All experimental procedures were approved by the Dalhousie University Committee on Laboratory Animals following the guidelines of the Canadian Council on Animal Care. Two groups of 5, 8-10 week old female C57/BL6 mice (Charles River Laboratories) were injected i.p with 3×10^6 ID8 shCTRL or ID8 shPRP4K cells, without specific randomization or blinding. The frequency of tumor nodules and tumor cells in the ascites was assessed 28 days later.

Ascites flow cytometry assay

Ascites fluid was isolated via peritoneal wash and red blood cell lysis was performed before flow cytometric analysis for GFP$^+$ ID8 cells. Data acquisition and analysis were performed using a two-laser FACSCalibur with Cell Quest Pro software (BD Biosciences).

Statistical analyses

For animal studies, an unpaired *T*-test was used; where an s.d. of 10% was assumed and 5 animals per group was expected to detect a 20% difference with a power of 0.8 (StatMate 2.00 by GraphPad, La Jolla, CA, USA). Normality of data was determined by Shapiro–Wilk test (http://sdittami.altervista.org/shapirotest/ShapiroTest.html). Kaplan–Meier curve analysis and Student's *T*-test (2-sided) were carried out using GraphPad Prism 7.03. Statistical significance was set at $P = 0.05$.

CONFLICT OF INTEREST

The authors declare no conflict of interest.

ACKNOWLEDGEMENTS

We thank the Gynecology-Oncology and Pathology services of the CHUM-Hôpital Notre-Dame for tumor procurement, Gretchen Wagner for fish care, and Monique Bernard for technical assistance. Ovarian and breast tumor banking was supported by the Cancer Research Network Tissue Bank of the Fonds de recherche du Québec—Santé (FRQS). This work was funded by research grants from the Canadian Breast Cancer Foundation (CBCF) and the Breast Cancer Society/QEII Foundation awarded to GD, and research grants to BJ from the Canadian Institutes of Health Research (CIHR) (MOP-110988, PJT-153285). GD, JB and BJ are Senior Scientists of the Beatrice Hunter Cancer Research Institute (BHCRI), and DPC, LC, JS and JP were supported by trainee awards from the BHCRI with funds provided by CBCF—Atlantic, The Canadian Cancer Society, Nova Scotia Division as part of The Terry Fox Foundation Strategic Health Research Training (STIHR) Program in Cancer Research at the CIHR. SG is the recipient of doctoral awards from the Killam Trusts, CIHR, and BHCRI.

REFERENCES

1 Frisch SM, Francis H. Disruption of epithelial cell-matrix interactions induces apoptosis. *J Cell Biol* 1994; **124**: 619–626.
2 Frisch SM, Ruoslahti E. Integrins and anoikis. *Curr Opin Cell Biol* 1997; **9**: 701–706.
3 Giancotti FG. Complexity and specificity of integrin signalling. *Nat Cell Biol* 2000; **2**: E13–E14.
4 Gabarra-Niecko V, Schaller MD, Dunty JM. FAK regulates biological processes important for the pathogenesis of cancer. *Cancer Metastasis Rev* 2003; **22**: 359–374.
5 Moro L, Venturino M, Bozzo C, Silengo L, Altruda F, Beguinot L *et al.* Integrins induce activation of EGF receptor: role in MAP kinase induction and adhesion-dependent cell survival. *EMBO J* 1998; **17**: 6622–6632.
6 Reginato MJ, Mills KR, Paulus JK, Lynch DK, Sgroi DC, Debnath J *et al.* Integrins and EGFR coordinately regulate the pro-apoptotic protein Bim to prevent anoikis. *Nat Cell Biol* 2003; **5**: 733–740.
7 Grassian AR, Schafer ZT, Brugge JS. ErbB2 stabilizes epidermal growth factor receptor (EGFR) expression via Erk and Sprouty2 in extracellular matrix-detached cells. *J Biol Chem* 2011; **286**: 79–90.
8 Rosenberg GH, Alahari SK, Kaufer NF. prp4 from *Schizosaccharomyces pombe*, a mutant deficient in pre-mRNA splicing isolated using genes containing artificial introns. *Mol Gen Genet* 1991; **226**: 305–309.
9 Dellaire G, Makarov EM, Cowger JM, Longman D, Sutherland HGE, Luhrmann R *et al.* Mammalian PRP4 kinase copurifies and interacts with components of both the U5 snRNP and the N-CoR deacetylase complexes. *Mol Cell Biol* 2002; **22**: 5141–5156.
10 Corkery DP, Le Page C, Meunier L, Provencher D, Mes-Masson AM, Dellaire G. PRP4K is a HER2-regulated modifier of taxane sensitivity. *Cell Cycle* 2015; **14**: 1059–1069.
11 Kojima T, Zama T, Wada K, Onogi H, Hagiwara M. Cloning of human PRP4 reveals interaction with Clk1. *J Biol Chem* 2001; **276**: 32247–32256.
12 Montembault E, Dutertre S, Prigent C, Giet R. PRP4 is a spindle assembly checkpoint protein required for MPS1, MAD1, and MAD2 localization to the kinetochores. *J Cell Biol* 2007; **179**: 601–609.
13 Schneider M, Hsiao HH, Will CL, Giet R, Urlaub H, Luhrmann R. Human PRP4 kinase is required for stable tri-snRNP association during spliceosomal B complex formation. *Nat Struct Mol Biol* 2010; **17**: 216–221.
14 Lam AJ, St-Pierre F, Gong Y, Marshall JD, Cranfill PJ, Baird MA *et al.* Improving FRET dynamic range with bright green and red fluorescent proteins. *Nat Methods* 2012; **9**: 1005–1012.
15 Zerial M, McBride H. Rab proteins as membrane organizers. *Nat Rev Mol Cell Biol* 2001; **2**: 107–117.
16 Pankiv S, Clausen TH, Lamark T, Brech A, Bruun JA, Outzen H *et al.* p62/SQSTM1 binds directly to Atg8/LC3 to facilitate degradation of ubiquitinated protein aggregates by autophagy. *J Biol Chem* 2007; **282**: 24131–24145.

17 Christoforidis S, McBride HM, Burgoyne RD, Zerial M. The Rab5 effector EEA1 is a core component of endosome docking. *Nature* 1999; **397**: 621–625.
18 Eskelinen EL, Tanaka Y, Saftig P. At the acidic edge: emerging functions for lysosomal membrane proteins. *Trends Cell Biol* 2003; **13**: 137–145.
19 Wiley HS, Herbst JJ, Walsh BJ, Lauffenburger DA, Rosenfeld MG, Gill GN. The role of tyrosine kinase activity in endocytosis, compartmentation, and down-regulation of the epidermal growth factor receptor. *J Biol Chem* 1991; **266**: 11083–11094.
20 Tomas A, Futter CE, Eden ER. EGF receptor trafficking: consequences for signaling and cancer. *Trends Cell Biol* 2014; **24**: 26–34.
21 Scharaw S, Iskar M, Ori A, Boncompain G, Laketa V, Poser I *et al.* The endosomal transcriptional regulator RNF11 integrates degradation and transport of EGFR. *J Cell Biol* 2016; **215**: 543–558.
22 Earp HS, Austin KS, Blaisdell J, Rubin RA, Nelson KG, Lee LW *et al.* Epidermal growth factor (EGF) stimulates EGF receptor synthesis. *J Biol Chem* 1986; **261**: 4777–4780.
23 Jost M, Huggett TM, Kari C, Rodeck U. Matrix-independent survival of human keratinocytes through an EGF receptor/MAPK-kinase-dependent pathway. *Mol Biol Cell* 2001; **12**: 1519–1527.
24 Douma S, Van Laar T, Zevenhoven J, Meuwissen R, Van Garderen E, Peeper DS. Suppression of anoikis and induction of metastasis by the neurotrophic receptor TrkB. *Nature* 2004; **430**: 1034–1039.
25 Smit MA, Peeper DS. Zeb1 is required for TrkB-induced epithelial-mesenchymal transition, anoikis resistance and metastasis. *Oncogene* 2011; **30**: 3735–3744.
26 Smit MA, Geiger TR, Song JY, Gitelman I, Peeper DS. A Twist-Snail axis critical for TrkB-induced epithelial-mesenchymal transition-like transformation, anoikis resistance, and metastasis. *Mol Cell Biol* 2009; **29**: 3722–3737.
27 Corkery DP, Dellaire G, Berman JN. Leukaemia xenotransplantation in zebrafish–chemotherapy response assay *in vivo*. *Br J Haematol* 2011; **153**: 786–789.
28 Tan DS, Agarwal R, Kaye SB. Mechanisms of transcoelomic metastasis in ovarian cancer. *Lancet Oncol* 2006; **7**: 925–934.
29 Cai Q, Yan L, Xu Y. Anoikis resistance is a critical feature of highly aggressive ovarian cancer cells. *Oncogene* 2014; **34**: 3315–3324.
30 Paoli P, Giannoni E, Chiarugi P. Anoikis molecular pathways and its role in cancer progression. *Biochim Biophys Acta* 2013; **1833**: 3481–3498.
31 Rosen K, Coll ML, Li A, Filmus J. Transforming growth factor-alpha prevents detachment-induced inhibition of c-Src kinase activity, Bcl-XL down-regulation, and apoptosis of intestinal epithelial cells. *J Biol Chem* 2001; **276**: 37273–37279.
32 Giannoni E, Buricchi F, Grimaldi G, Parri M, Cialdai F, Taddei ML *et al.* Redox regulation of anoikis: reactive oxygen species as essential mediators of cell survival. *Cell Death Differ* 2008; **15**: 867–878.
33 Wang Y, Pennock S, Chen X, Wang Z. Endosomal signaling of epidermal growth factor receptor stimulates signal transduction pathways leading to cell survival. *Mol Cell Biol* 2002; **22**: 7279–7290.
34 Alanko J, Mai A, Jacquemet G, Schauer K, Kaukonen R, Saari M *et al.* Integrin endosomal signalling suppresses anoikis. *Nat Cell Biol* 2015; **17**: 1412–1421.
35 Nguyen LN, Holdren MS, Nguyen AP, Furuya MH, Bianchini M, Levy E *et al.* Sorting nexin 1 down-regulation promotes colon tumorigenesis. *Clin Cancer Res* 2006; **12**: 6952–6959.
36 Martin MJ, Melnyk N, Pollard M, Bowden M, Leong H, Podor TJ *et al.* The insulin-like growth factor I receptor is required for Akt activation and suppression of anoikis in cells transformed by the ETV6-NTRK3 chimeric tyrosine kinase. *Mol Cell Biol* 2006; **26**: 1754–1769.
37 Khwaja A, Rodriguez-Viciana P, Wennstrom S, Warne PH, Downward J. Matrix adhesion and Ras transformation both activate a phosphoinositide 3-OH kinase and protein kinase B/Akt cellular survival pathway. *EMBO J* 1997; **16**: 2783–2793.
38 Wang P, Zhou Z, Hu A, Ponte de Albuquerque C, Zhou Y, Hong L *et al.* Both decreased and increased SRPK1 levels promote cancer by interfering with PHLPP-mediated dephosphorylation of Akt. *Mol Cell* 2014; **54**: 378–391.
39 Gross T, Lutzelberger M, Weigmann H, Klingenhoff A, Shenoy S, Kaufer NF. Functional analysis of the fission yeast Prp4 protein kinase involved in pre-mRNA splicing and isolation of a putative mammalian homologue. *Nucleic Acids Res* 1997; **25**: 1028–1035.
40 Gui JF, Lane WS, Fu XD. A serine kinase regulates intracellular localization of splicing factors in the cell cycle. *Nature* 1994; **369**: 678–682.
41 Kataoka N, Bachorik JL, Dreyfuss G. Transportin-SR, a nuclear import receptor for SR proteins. *J Cell Biol* 1999; **145**: 1145–1152.
42 Lai MC, Lin RI, Tarn WY. Transportin-SR2 mediates nuclear import of phosphorylated SR proteins. *Proc Natl Acad Sci USA* 2001; **98**: 10154–10159.
43 Lai MC, Lin RI, Huang SY, Tsai CW, Tarn WY. A human importin-beta family protein, transportin-SR2, interacts with the phosphorylated RS domain of SR proteins. *J Biol Chem* 2000; **275**: 7950–7957.
44 Gui JF, Tronchere H, Chandler SD, Fu XD. Purification and characterization of a kinase specific for the serine- and arginine-rich pre-mRNA splicing factors. *Proc Natl Acad Sci USA* 1994; **91**: 10824–10828.
45 Ayantunde AA, Parsons SL. Pattern and prognostic factors in patients with malignant ascites: a retrospective study. *Ann Oncol* 2007; **18**: 945–949.
46 Ahmed N, Stenvers KL. Getting to know ovarian cancer ascites: opportunities for targeted therapy-based translational research. *Front Oncol* 2013; **3**: 256.
47 Garrison RN, Kaelin LD, Galloway RH, Heuser LS. Malignant ascites. Clinical and experimental observations. *Ann Surg* 1986; **203**: 644–651.
48 Parsons SL, Lang MW, Steele RJ. Malignant ascites: a 2-year review from a teaching hospital. *Eur J Surg Oncol* 1996; **22**: 237–239.
49 Adam RA, Adam YG. Malignant ascites: past, present, and future. *J Am Coll Surg* 2004; **198**: 999–1011.
50 Feldman GB, Knapp RC, Order SE, Hellman S. The role of lymphatic obstruction in the formation of ascites in a murine ovarian carcinoma. *Cancer Res* 1972; **32**: 1663–1666.
51 Bookman MA, McGuire WP 3rd, Kilpatrick D, Keenan E, Hogan WM, Johnson SW *et al.* Carboplatin and paclitaxel in ovarian carcinoma: a phase I study of the Gynecologic Oncology Group. *J Clin Oncol* 1996; **14**: 1895–1902.
52 McGuire WP, Hoskins WJ, Brady MF, Kucera PR, Partridge EE, Look KY *et al.* Cyclophosphamide and cisplatin compared with paclitaxel and cisplatin in patients with stage III and stage IV ovarian cancer. *N Engl J Med* 1996; **334**: 1–6.
53 Ozols RF, Bundy BN, Greer BE, Fowler JM, Clarke-Pearson D, Burger RA *et al.* Phase III trial of carboplatin and paclitaxel compared with cisplatin and paclitaxel in patients with optimally resected stage III ovarian cancer: a Gynecologic Oncology Group study. *J Clin Oncol* 2003; **21**: 3194–3200.
54 Herzog TJ. Recurrent ovarian cancer: how important is it to treat to disease progression? *Clin Cancer Res* 2004; **10**: 7439–7449.
55 Markman M, Rowinsky E, Hakes T, Reichman B, Jones W, Lewis JL Jr *et al.* Phase I trial of intraperitoneal taxol: a Gynecoloic Oncology Group study. *J Clin Oncol* 1992; **10**: 1485–1491.
56 Cancer Genome Atlas Research N, Integrated genomic analyses of ovarian carcinoma. *Nature* 2011; **474**: 609–615.
57 Letourneau IJ, Quinn MC, Wang LL, Portelance L, Caceres KY, Cyr L *et al.* Derivation and characterization of matched cell lines from primary and recurrent serous ovarian cancer. *BMC Cancer* 2012; **12**: 379.
58 Le Page C, Marineau A, Bonza PK, Rahimi K, Cyr L, Labouba I *et al.* BTN3A2 expression in epithelial ovarian cancer is associated with higher tumor infiltrating T cells and a better prognosis. *PloS One* 2012; **7**: e38541.
59 Roby KF, Taylor CC, Sweetwood JP, Cheng Y, Pace JL, Tawfik O *et al.* Development of a syngeneic mouse model for events related to ovarian cancer. *Carcinogenesis* 2000; **21**: 585–591.
60 Bedard K, Attar H, Bonnefont J, Jaquet V, Borel C, Plastre O *et al.* Three common polymorphisms in the CYBA gene form a haplotype associated with decreased ROS generation. *Hum Mutat* 2009; **30**: 1123–1133.
61 Pinder J, Salsman J, Dellaire G. Nuclear domain 'knock-in' screen for the evaluation and identification of small molecule enhancers of CRISPR-based genome editing. *Nucleic acids Res* 2015; **43**: 9379–9392.
62 Cong L, Ran FA, Cox D, Lin S, Barretto R, Habib N *et al.* Multiplex genome engineering using CRISPR/Cas systems. *Science* 2013; **339**: 819–823.
63 Franken NA, Rodermond HM, Stap J, Haveman J, van Bree C. Clonogenic assay of cells *in vitro*. *Nat Protoc* 2006; **1**: 2315–2319.
64 Gebremeskel S, Clattenburg DR, Slauenwhite D, Lobert L, Johnston B. Natural killer T cell activation overcomes immunosuppression to enhance clearance of postsurgical breast cancer metastasis in mice. *Oncoimmunology* 2015; **4**: e995562.
65 Gao J, Aksoy BA, Dogrusoz U, Dresdner G, Gross B, Sumer SO *et al.* Integrative analysis of complex cancer genomics and clinical profiles using the cBioPortal. *Sci Signal* 2013; **6**: pl1.

Supplementary Information accompanies this paper on the Oncogene website (http://www.nature.com/onc)